

Supporting Information for:

Synergistic effect of mixed-ligands on anisotropy axis of two dinuclear dysprosium complexes

Hongshan Ke,^{*a} Yongsheng Yang,^a Wen Wei,^a Youdong Jiang,^a Yi-Quan Zhang,^{*b} Gang Xie^a and Sanping Chen^{*a}

^aKey Laboratory of Synthetic and Natural Functional Molecule of the Ministry of Education, College of Chemistry and Materials Science, Northwest University, Xi'an 710069, P. R. China. Email: hske@nwu.edu.cn, sanpingchen@126.com

^bJiangsu Key Laboratory for NSLSCS, School of Physical Science and Technology, Nanjing Normal University, Nanjing 210023, P. R. China. E-mail: zhangyiquan@njnu.edu.cn

Table S1 *SHAPE*¹ analyses of compounds **1** and **2**

Configuration	Dy1	Dy2
Octagon(D _{8h})	30.356(31.031)	29.682(31.305)
Heptagonal pyramid(C _{7v})	23.032(23.879)	23.371(22.897)
Hexagonal bipyramid(D _{6h})	16.150(14.711)	15.372(15.232)
Cube(O _h)	10.032(9.071)	9.012(8.730)
Square antiprism(D _{4d})	2.527(3.172)	1.991(2.379)
Triangular dodecahedron(D_{2d})	1.097(1.043)	1.203(0.942)
Johnson gyrobifastigium J26(D _{2d})	13.799(14.254)	14.420(14.329)
Johnson elongated triangular bipyramid J14(D _{3h})	26.388(25.935)	25.243(27.038)
Biaugmented trigonal prism J50(C _{2v})	2.504(2.661)	2.530(2.823)
Biaugmented trigonal prism(C _{2v})	2.473(2.547)	2.535(2.735)
Snub diphenoïd J84(D _{2d})	2.445(2.622)	2.729(2.734)
Triakis tetrahedron(T _d)	10.340(9.403)	9.302(9.091)
Elongated trigonal bipyramid(D _{3h})	22.302(21.171)	20.401(22.463)

Note: the values in the bracket represent the coordination geometry result of compound **2**.

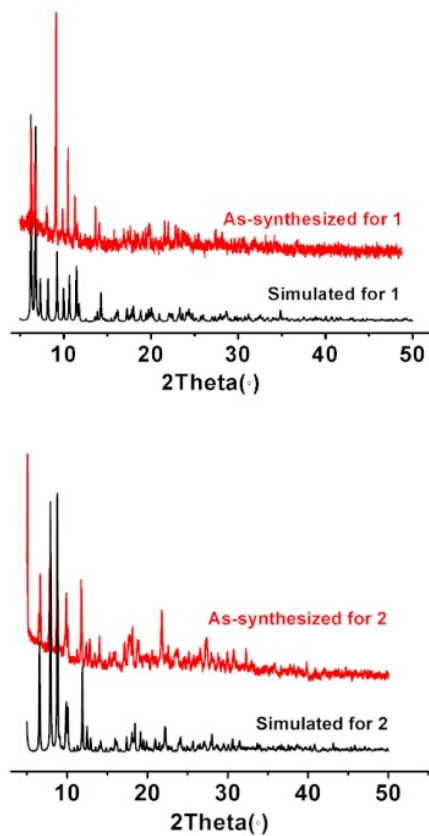


Fig. S1 Comparing the simulated PXRD (black) and experimental patterns (red) of complexes **1** (top) and **2** (bottom).

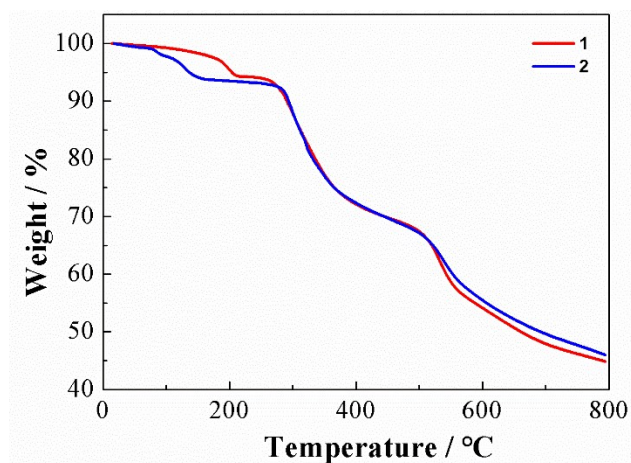


Fig. S2 The TGA plots for complexes **1** (red lines) and **2** (blue lines).

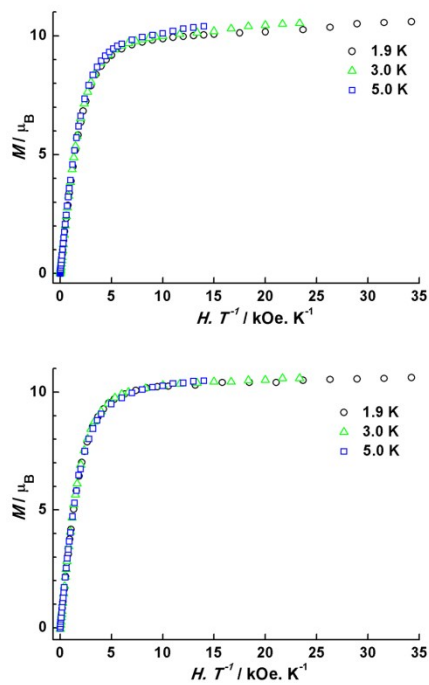


Fig. S3 Field dependence of the reduced magnetization data for complexes **1** (top) and **2** (bottom) at 1.9, 3, and 5 K.

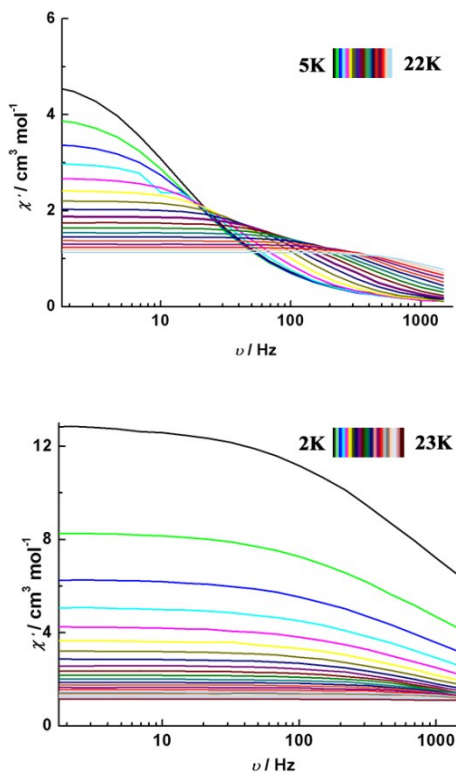


Fig. S4 Frequency dependence of the in-phase (χ') ac magnetic susceptibility data for **1** (top) and **2** (bottom) under zero applied dc field.

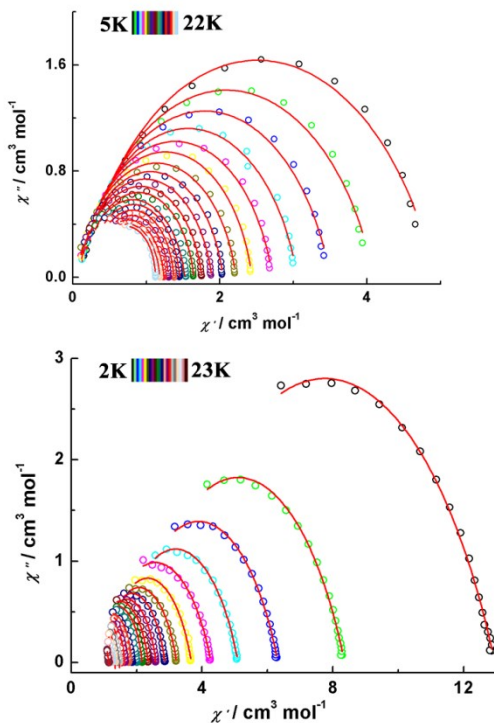


Fig. S5 Cole-Cole² plots for ac susceptibility collected under zero applied dc field for **1** (top) and **2** (bottom). Red solid lines represent the fits to the data.

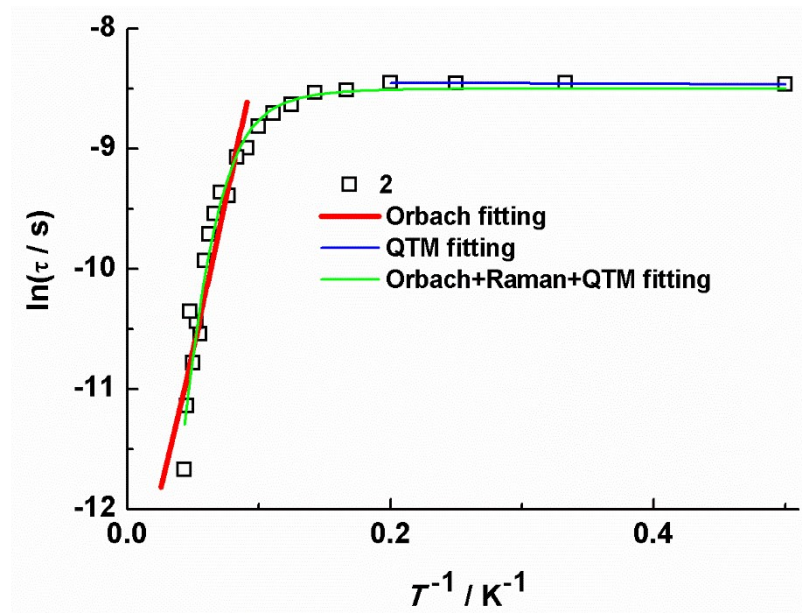


Fig. S6 $\ln(\tau)$ vs. T^{-1} plots for **2** (hollow squares, 2-23 K).

Table S2 χ_T , χ_S , τ and α values of **1** and **2** estimated by theoretical calculations on the basis of the generalized Debye³ model

	1							
T/K	5	6	7	8	9	10	11	12
$\chi_T/\text{cm}^3 \text{ mol}^{-1}$	4.946	4.116	3.519	3.069	2.730	2.454	2.234	2.058
$\chi_S/\text{cm}^3 \text{ mol}^{-1}$	0.12	0.11	0.11	0.089	0.085	0.086	0.0679	0.073
$\tau/\mu\text{sec}$	10170	7940	5990	4400	3120	2200	1560	1130
α	0.236	0.214	0.191	0.184	0.163	0.149	0.152	0.154
T/K	13	14	15	16	17	18	19	20
$\chi_T/\text{cm}^3 \text{ mol}^{-1}$	1.901	1.769	1.657	1.553	1.463	1.381	1.306	1.242
$\chi_S/\text{cm}^3 \text{ mol}^{-1}$	0.070	0.072	0.105	0.108	0.147	0.197	0.250	0.266
$\tau/\mu\text{sec}$	824	606	470	354	281	229	188	149
α	0.151	0.155	0.147	0.145	0.147	0.115	0.088	0.084
T/K	21	22						
$\chi_T/\text{cm}^3 \text{ mol}^{-1}$	1.182	1.123						
$\chi_S/\text{cm}^3 \text{ mol}^{-1}$	0.308	0.297						
$\tau/\mu\text{sec}$	122	92.9						
α	0.056	0.045						
	2							
T/K	2	3	4	5	6	7	8	9
$\chi_T/\text{cm}^3 \text{ mol}^{-1}$	12.98	8.37	6.34	5.11	4.29	3.68	3.23	2.88
$\chi_S/\text{cm}^3 \text{ mol}^{-1}$	2.52	1.74	1.37	1.21	0.78	0.94	0.84	0.78
τ/sec	211	214	213	214	201	197	178	166
α	0.376	0.363	0.353	0.340	0.350	0.310	0.300	0.270
T/K	10	11	12	13	14	15	16	17
$\chi_T/\text{cm}^3 \text{ mol}^{-1}$	2.59	2.36	2.17	2.01	1.87	1.75	1.65	1.55
$\chi_S/\text{cm}^3 \text{ mol}^{-1}$	0.71	0.59	0.62	0.45	0.54	0.52	0.50	0.38
$\tau/\mu\text{sec}$	149	124	115	83.3	86.0	71.8	60.5	48.4
α	0.254	0.234	0.208	0.232	0.189	0.178	0.180	0.177
T/K	18	19	20	21	22	23		
$\chi_T/\text{cm}^3 \text{ mol}^{-1}$	1.47	1.39	1.32	1.26	1.20	1.15		
$\chi_S/\text{cm}^3 \text{ mol}^{-1}$	0.36	0.20	0.18	0.48	0.12	0.15		
$\tau/\mu\text{sec}$	26.4	29.2	20.7	31.8	14.5	8.55		
α	0.198	0.179	0.194	0.163	0.168	0.229		

Table S3 χ_T , χ_S , and α parameters of **1** and **2** derived from Cole-Cole² fitting

1								
T/K	5	6	7	8	9	10	11	12
$\chi_T/\text{cm}^3 \text{ mol}^{-1}$	4.924	4.097	3.498	3.051	2.713	2.438	2.221	2.042
$\chi_S/\text{cm}^3 \text{ mol}^{-1}$	0.097	0.086	0.09	0.088	0.071	0.080	0.058	0.078
α	0.241	0.220	0.193	0.175	0.160	0.140	0.144	0.133
T/K	13	14	15	16	17	18	19	20
$\chi_T/\text{cm}^3 \text{ mol}^{-1}$	1.888	1.756	1.644	1.521	1.453	1.372	1.300	1.239
$\chi_S/\text{cm}^3 \text{ mol}^{-1}$	0.080	0.086	0.145	0.110	0.206	0.257	0.297	0.274
α	0.127	0.125	0.101	0.119	0.082	0.062	0.0481	0.071
T/K	21	22						
$\chi_T/\text{cm}^3 \text{ mol}^{-1}$	1.180	1.125						
$\chi_S/\text{cm}^3 \text{ mol}^{-1}$	0.312	0.350						
α	0.050	0.047						
2								
T/K	2	3	4	5	6	7	8	9
$\chi_T/\text{cm}^3 \text{ mol}^{-1}$	12.95	8.35	6.32	5.10	4.27	3.67	3.22	2.87
$\chi_S/\text{cm}^3 \text{ mol}^{-1}$	2.56	1.85	1.47	1.28	0.87	1.00	0.93	0.85
α	0.37	0.349	0.337	0.326	0.331	0.291	0.27	0.24
T/K	10	11	12	13	14	15	16	17
$\chi_T/\text{cm}^3 \text{ mol}^{-1}$	2.58	2.36	2.17	2.01	1.85	1.75	1.64	1.55
$\chi_S/\text{cm}^3 \text{ mol}^{-1}$	0.81	0.63	0.67	0.48	0.66	0.51	0.68	0.27
α	0.22	0.22	0.186	0.216	0.13	0.177	0.12	0.20
T/K	18	19	20	21	22	23		
$\chi_T/\text{cm}^3 \text{ mol}^{-1}$	1.47	1.39	1.33	1.26	1.2	1.15		
$\chi_S/\text{cm}^3 \text{ mol}^{-1}$	0.3	0.28	0.24	0.42	0.1	0.17		
α	0.194	0.215	0.257	0.174	0.20	0.235		

Table S4 Calculated energy levels (cm^{-1}), \mathbf{g} (g_x, g_y, g_z) tensors and m_J values of the lowest eight Kramers doublets (KDs) of individual Dy^{III} fragments with respect to the pseudospin $\frac{S}{2} = 1/2$ in complexes **1** and **2** using CASSCF/RASSI with MOLCAS 8.2⁴

1						
KDs	Dy1			Dy2		
	E/cm^{-1}	\mathbf{g}	m_J	E/cm^{-1}	\mathbf{g}	m_J
1	0.0	0.003			0.006	
		0.004	$\pm 15/2$	0.0	0.008	$\pm 15/2$
		19.665			19.709	
2	224.8	0.114			0.218	
		0.226	$\pm 13/2$	221.5	0.419	$\pm 13/2$
		15.897			16.132	
3	331.8	0.337			0.767	
		0.485	$\pm 11/2$	325.6	1.051	$\pm 11/2$
		13.451			13.571	
4	435.6	0.661			0.197	
		1.632	$\pm 9/2$	413.8	1.818	$\pm 9/2$
		9.964			9.709	
5	525.6	5.326			4.897	
		5.487	$\pm 7/2$	493.2	5.980	$\pm 5/2$
		7.968			9.005	

		1.287			0.731	
6	578.8	2.639	$\pm 3/2$	562.0	1.401	$\pm 1/2$
		15.753			14.488	
		0.234			0.078	
7	662.6	0.358	$\pm 1/2$	647.0	0.117	$\pm 3/2$
		16.813			18.952	
		0.069			0.005	
8	747.6	0.137	$\pm 5/2$	732.5	0.017	$\pm 7/2$
		18.803			19.453	

2

KDs	Dy1			Dy2		
	E/cm^{-1}	\mathbf{g}	m_J	E/cm^{-1}	\mathbf{g}	m_J
1	0.0	0.016 0.027 19.578	$\pm 15/2$	0.0	0.001 0.001 19.667	$\pm 15/2$
2	208.7	0.566 1.309 15.141	$\pm 13/2$	226.0	0.014 0.022 16.272	$\pm 13/2$
3	293.0	0.689 1.954 12.829	$\pm 11/2$	367.4	0.445 0.690 13.323	$\pm 11/2$

		1.383			2.130	
4	386.7	4.513	$\pm 9/2$	462.7	2.501	$\pm 9/2$
		9.389			9.546	
5	464.7	3.562			4.805	
		6.029	$\pm 5/2$	560.9	5.304	$\pm 7/2$
6	546.1	10.346			8.772	
		0.126			0.916	
7	633.9	0.339	$\pm 1/2$	644.5	1.729	$\pm 3/2$
		15.044			15.264	
8	683.2	0.132			0.190	
		0.225	$\pm 3/2$	701.8	0.305	$\pm 1/2$
		17.938			17.305	
		0.046			0.129	
		0.122	$\pm 7/2$	769.6	0.190	$\pm 5/2$
		18.798			18.384	

Table S5 Wave functions with definite projection of the total moment $|m_J\rangle$ for the lowest KDs of individual Dy^{III} fragments for complexes **1** and **2** using CASSCF/RASSI-SO with MOLCAS 8.2⁴

1		
	E/cm ⁻¹	Wave functions
Dy1	0.0	96% ±15/2>
	224.8	80% ±13/2>+16% ±9/2>
Dy2	0.0	97% ±15/2>
	221.5	83% ±13/2>+14% ±9/2>

2		
	E/cm ⁻¹	Wave functions
Dy1	0.0	96% ±15/2>
	208.7	73% ±13/2>+18% ±9/2>
Dy2	0.0	96% ±15/2>
	226.0	83% ±13/2>+14% ±9/2>
	367.4	52% ±11/2>+30% ±7/2>

Table S6 Fitted exchange coupling J_{exch} , the calculated dipole-dipole interaction J_{dip} and the calculated total constant J_{total} of magnetic centers in **1** and **2** (cm⁻¹). The intermolecular interaction zJ' was fitted to -0.03 and -0.01 cm⁻¹, respectively

	1	2
J_{dip}	0.71	1.19
J_{exch}	-3.25	-3.25
J_{total}	-2.54	-2.06

Table S7 Exchange energies E (cm^{-1}), the energy difference between each exchange doublets Δ_t (cm^{-1}) and the main values of the g_z for the lowest two exchange doublets of **1** and **2**.

	E	Δ_t	g_z
1			
1	0.0	3.94×10^{-6}	23.020
2	0.1	4.17×10^{-6}	31.943
2			
1	0.0	2.48×10^{-5}	21.299
2	0.2	2.50×10^{-5}	32.747

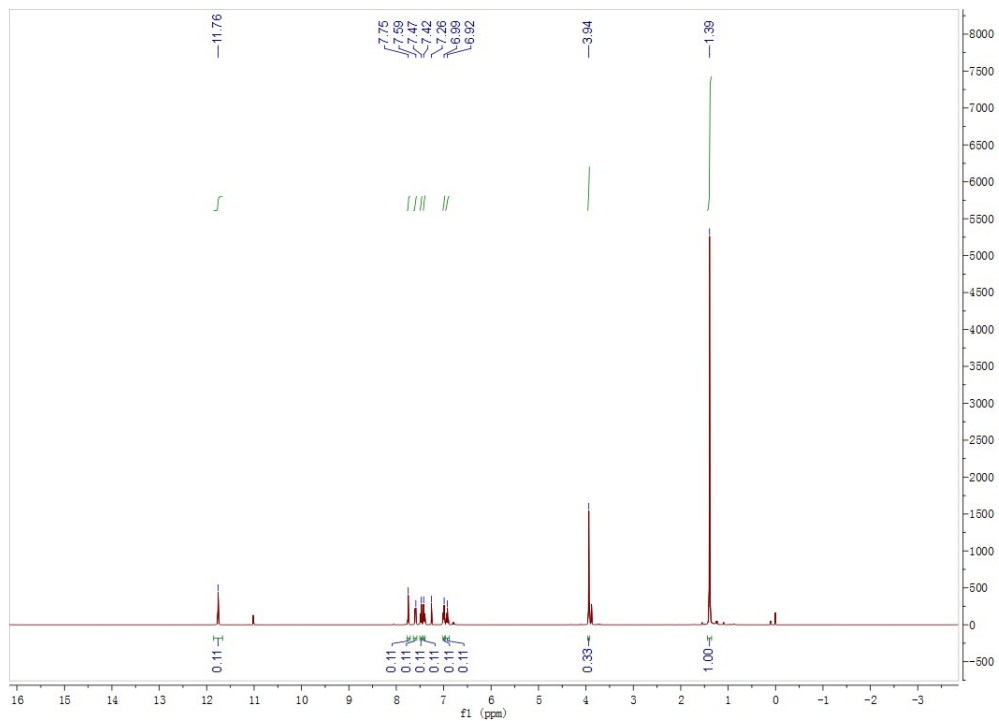


Figure S7 ^1H NMR spectra of the ligand HL_3 (400 MHz, CDCl_3 , 298 K).

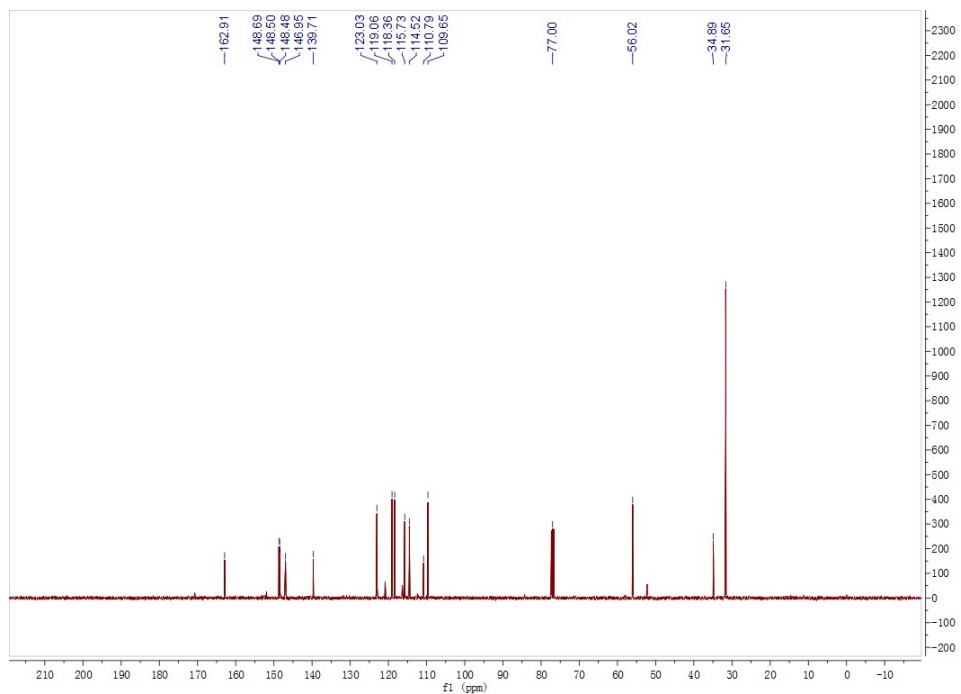


Figure S8 ^{13}C NMR spectra of the ligand HL_3 (400 MHz, CDCl_3 , 298 K).

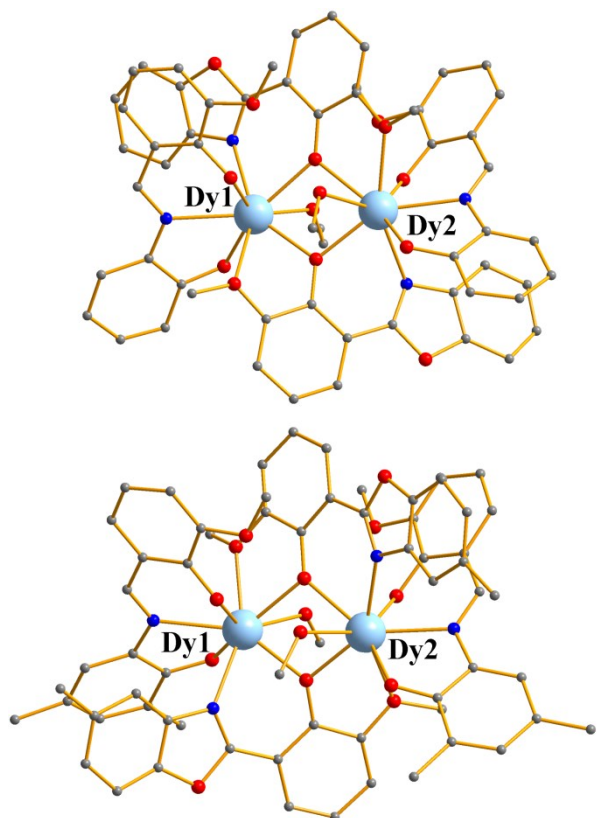


Figure S9 Calculated core structure of **1** (top) and **2** (bottom). H atoms are omitted. The tert-butyl groups in **1** and the methyl groups of each tert-butyl group in **2** are removed.

Table S8 Crystal data and structure refinements for **1** and **2**

Compound	1	2
Empirical formula	C ₉₁ H ₁₁₆ Dy ₂ N ₄ O ₁₄	C _{83.5} H ₁₀₄ Dy ₂ N ₄ O _{15.5}
Formula weight	1814.87	1736.70
Temperature (K)	296.98	150
Crystal system	trigonal	tetragonal
Space group	R3	I4 ₁ /a
a (Å)	26.065(3)	40.7539(19)
b (Å)	26.065(3)	40.7539(19)
c (Å)	36.149(6)	20.1854(9)
α (°)	90	90
β (°)	90	90
γ (°)	120	90
Volume (Å ³)	21268(6)	33526(3)
Z	9	16
F(000)	8406.0	14224.0
ρ _{calg} /cm ³	1.275	1.376
μ/mm ⁻¹	8.827	1.833
Radiation	CuKα	MoK\α
Reflections collected	20461	121120
Independent reflections	10693	15945
Data/restraints/parameters	10693/894/1129	15945/88/1045
Goodness of fit on (F ²)	1.185	1.068
Final R indexes [I>=2σ (I)]	R ₁ = 0.0595 wR ₂ = 0.1585	R ₁ = 0.0505 wR ₂ = 0.1004
R indexes (all data)	R ₁ = 0.0728 wR ₂ = 0.1663	R ₁ = 0.0872 wR ₂ = 0.1163
Largest diff. peak/hole / e Å ⁻³	0.88/-0.50	1.18/-1.32

Table S9 Selected bond lengths (\AA) and angles ($^\circ$) for **1** and **2**

	1	2	
Bond lengths (\AA)			
Dy(1)-N(2)	2.487(11)	Dy(1)-N(2)	2.529(5)
Dy(1)-N(3)	2.497(13)	Dy(1)-N(3)	2.491(5)
Dy(1)-O(1)	2.595(11)	Dy(1)-O(1)	2.428(4)
Dy(1)-O(2)	2.308(9)	Dy(1)-O(2)	2.376(4)
Dy(1)-O(5)	2.392(10)	Dy(1)-O(5)	2.315(4)
Dy(1)-O(8)	2.239(11)	Dy(1)-O(8)	2.251(4)
Dy(1)-O(9)	2.222(10)	Dy(1)-O(9)	2.211(4)
Dy(1)-O(13)	2.490(10)	Dy(1)-O(14)	2.497(4)
Dy(2)-N(1)	2.543(13)	Dy(2)-N(1)	2.481(5)
Dy(2)-N(4)	2.484(12)	Dy(2)-N(4)	2.468(5)
Dy(2)-O(2)	2.298(9)	Dy(2)-O(2)	2.360(4)
Dy(2)-O(4)	2.465(11)	Dy(2)-O(4)	2.609(4)
Dy(2)-O(5)	2.401(10)	Dy(2)-O(5)	2.328(4)
Dy(2)-O(11)	2.206(11)	Dy(2)-O(11)	2.228(4)
Dy(2)-O(12)	2.213(10)	Dy(2)-O(12)	2.188(4)
Dy(2)-O(14)	2.517(10)	Dy(2)-O(13)	2.462(4)
Bond angles ($^\circ$)			
Dy(1)-O(2)-Dy(2)	108.8(4)	Dy(1)-O(2)-Dy(2)	103.77(16)
Dy(1)-O(5)-Dy(2)	102.7(4)	Dy(1)-O(5)-Dy(2)	106.75(16)

References

- 1 D. Casanova, M. Llunell, P. Alemany and S. Alvarez, *Chem. -Eur. J.*, 2005, **11**, 1479.
- 2 K. S. Cole and R. H. Cole, *J. Chem. Phys.*, 1941, **9**, 341.
- 3 S. M. J. Aubin, Z. Sun, L. Pardi, J. Krzystek, K. Folting, L.-C. Brunel, A. L. Rheingold, G. Christou and D. N. Hendrickson, *Inorg. Chem.*, 1999, **38**, 5329.
- 4 a) V. Veryzov, P.-O. Widmark, L. Serrano-Andrés, R. Lindh and B. O. Roos, *Int. J. Quantum. Chem.*, 2004, **100**, 626; b) G. Karlström, R. Lindh, P.-Å. Malmqvist, B. O. Roos, U. Ryde, V. Veryzov, P.-O. Widmark, M. Cossi, B. Schimmelpfennig, P. Neogrady and L. Seijo, *Comput. Mater. Sci.*, 2003, **28**,

222; c) F. Aquilante, L. d. Vico, N. Ferré, G. Ghigo, P.-Å. Malmqvist, P. NeogrÁdy, T. B. Pedersen, M. Pitoňák, M. Reiher, B. O. Roos, L. Serrano-Andrés, M. Urban, V. Veryazov and R. Lindh, *J. Comput. Chem.*, 2010, **31**, 224.